Structural Characterization of Pyridazine (pydz) Adducts of MX_2 (M = Mn, Fe, Co, Ni, Cu or Zn; X = Cl or Br). *Ab-initio* X-Ray Powder Diffraction Determination of Polymeric $[NiX_2(pydz)]$ Complexes†

Norberto Masciocchi,[*,a] **Paolo Cairati,**[a] **Lucia Carlucci,**[a] **Gianfranco Ciani,**[a] **Gianni Mezza**[b] **and Angelo Sironi**[*,a]
[a] *Istituto di Chimica Strutturistica Inorganica, Università di Milano, via Venezian 21, I 20133 Milano, Italy*
[b] *Centro C.N.R. di Studio sulla Sintesi e la Struttura dei Composti dei Metalli di Transizione nei Bassi Stati di Ossidazione, via Venezian 21, I 20133 Milano, Italy*

The pyridazine (pydz) complexes of metal halides MX_2 (M = Mn, Fe, Co, Ni, Cu or Zn; X = Cl or Br) have been prepared, using a reagent molar ratio of 1 : 1, and investigated by X-ray powder diffraction methods. The crystal structures (orthorhombic, space group *Imma*, $Z = 4$) of $[NiCl_2(pydz)]$ and $[NiBr_2(pydz)]$ have been determined, *ab initio*, from laboratory X-ray powder diffraction data only: $[NiCl_2(pydz)]$, $a = 7.3758(4)$, $b = 6.6069(3)$ and $c = 12.7292(7)$ Å, $[NiBr_2(pydz)]$, $a = 7.5598(9)$, $b = 6.8029(8)$ and $c = 12.905(2)$ Å. The structures have been solved by direct methods, and refined by the Rietveld technique down to R_{profile} values of 0.062 and 0.078, respectively, for 4400 data points collected at room temperature in the range $17 < 2\theta < 105°$. Both compounds consist of infinite polymeric chains of nickel atoms, bridged by X (Cl or Br) and pyridazine ligands, showing an octahedral arrangement and *trans*-D_{4h} NiX_4N_2 chromophores. The Ni–Cl and Ni–Br distances are 2.422(1) and 2.560(2) Å, respectively. Analyses of the other species have shown that the analogues of Mn, Fe and Co are isomorphous with the nickel compounds, while those of Cu and Zn display different diffraction patterns.

N-Donor heterocyclic rings with two or more nitrogen atoms display the ability to bond to different metal units, acting as '*exopolydentate*', rather than as '*endopolydentate*' ligands; they can form, therefore, oligo- and poly-meric metal complexes, with a variety of structural geometries.[1] These species are of interest for their potential role in multimetal-centred catalysis.[2] The polymers are particularly attractive in connection with material science, for their potential properties, such as electrical conductivity [*e.g.* in (phthalocyaninato)metal–pyrazine polymers[3]] and magnetism [see ref. 1(*a*) and refs. therein], especially as one- or two- and also as three-dimensional solids, in the tailoring of new phases, *e.g.* 'scaffolding-like materials',[4] an example of which, a copper(I)–pyrazine system, has recently been reported.[5]

Many investigations have so far been devoted to the adducts of pyridazine (1,2-diazine, hereafter indicated as pydz) with metal dihalides,[6–17] which are almost intractable solids, insoluble in the common organic solvents and, therefore, difficult to study with conventional techniques; most give powders or microcrystalline samples, unsuitable for single-crystal X-ray studies. The polymeric nature of the products was inferred by their insolubility and high stability, and hypothetical structures were proposed on the basis of far-IR data and of the low-temperature antiferromagnetic behaviour of the CuX_2 adducts (see refs. 10 and 13). In spite of the relevance of a detailed structural characterization for the interpretation of physical properties, no direct structural investigation was possible until recently (1990), when gel-permeation crystallization techniques made available single crystals of $[CuCl_2(pydz)]$,[18] suitable for conventional X-ray analysis.

In the last decade there has been a growing interest in powder diffraction methods for structural refinement of simple crystalline motifs, either by the Rietveld technique[19] or by the less popular 'two-stage' method.[20] The appearance and availability of high-flux, high-resolution sources (synchrotrons, neutron reactors and spallation sources) has favoured the rapid growth of new experimental[21] and numerical[22] techniques for *ab-initio* structure determination from powder diffraction data, initially performed on 'classical' inorganic compounds only.[23] More recently, the structures of a few organic[24] and organometallic[25] compounds have been unravelled by this method, and data obtained from standard laboratory equipment successfully used.

We have recently started a project on the use of laboratory X-ray powder diffraction (XRPD) to solve the crystal and molecular structure of metallorganic complexes failing to afford, for many reasons, single crystals of suitable size. Accordingly, the polymeric structures of $[\{Ru(CO)_4\}_n]$,[26] $[\{Cu(C_3H_3N_2)\}_n]$ (α and β forms), $[\{Ag(C_3H_3N_2)\}_n]$,[27] and the oligomeric nature of the $[\{HgRu(CO)_4\}_4]$[28] and $[\{Ag(C_3H_3N_2)\}_3]$[27] ($C_3H_4N_2$ = pyrazole) complexes were successfully characterized.

In this paper we report on the *ab-initio* structure determination, from laboratory XRPD data only, of the crystalline complexes $[NiCl_2(pydz)]$ **1** and $[NiBr_2(pydz)]$ **2**, which, in the solid state, form infinite chains of halide and μ-pydz-bridged nickel(II) ions. The corresponding adducts of the dihalides of Mn, Fe, Co, Cu and Zn with pydz have also been prepared and investigated by XRPD techniques, in order to attempt a structural classification of the whole family.

---

† *Supplementary data available* (No. SUP 57027, 25 pp.): remaining bond lengths and angles, reflection indices and intensities. See Instructions for Authors, *J. Chem. Soc., Dalton Trans.*, 1994, Issue 1, pp. xxiii–xxviii.

Non-SI unit employed: $\mu_B \approx 9.27 \times 10^{24}$ J T^{-1}.

Experimental

General Comments.—All the reagents and solvents employed were commercially available high-grade purity materials: pyridazine, $MnCl_2\cdot4H_2O$, $FeBr_2$, $CoCl_2\cdot6H_2O$, $NiCl_2\cdot6H_2O$, $NiBr_2\cdot3H_2O$, $CuCl_2\cdot2H_2O$, $CuBr_2$, $ZnCl_2$ (Fluka Chemie); $MnBr_2\cdot4H_2O$, $FeCl_2\cdot4H_2O$, $CoBr_2\cdot H_2O$, $ZnBr_2$ (Aldrich Chemical Co.). They were used as supplied, without further purification. Elemental analyses were carried out at the Microanalytical Laboratory of this University.

Physical Measurements.—Infrared spectra were recorded on a Perkin-Elmer 371 grating spectrophotometer (range 4000–600 cm^{-1}) in KBr pellets. Room-temperature magnetic susceptibilities were measured on a MSB-AUTO (Sherwood Scientific) magnetic balance. Diamagnetic corrections were estimated from Pascal's constants.

Syntheses.—All products were obtained by addition of pydz to an ethanolic solution of the appropriate salt at room temperature, in the molar ratio of 1 : 1. The preparation of $[NiCl_2(pydz)]$ is described, the syntheses of the other species being accomplished on the same lines.

$[NiCl_2(pydz)]$ **1**. Pyridazine (0.085 cm^3, 1.17 mmol) was added to an ethanolic solution (15 cm^3) of $NiCl_2\cdot6H_2O$ (0.278 g, 1.17 mmol). The colour immediately changed to pale blue and a precipitate rapidly separated. It was filtered off, washed with ethanol and dried in air (yield 74%) (Found: C, 23.35; H, 2.05; N, 13.40. Calc. for $C_4H_4Cl_2N_2Ni$: C, 22.90; H, 1.90; N, 13.35%). The green complex displays a μ_{eff} at 294 K of 3.1 μ_B. The main pydz IR bands (cm^{-1}) are at 1578s, 1454m, 1414s, 1074s, 1001s, 764vs and 684m.

The same product was obtained upon addition of pydz (0.175 cm^3, 2.41 mmol) to a water solution (10 cm^3) of the nickel salt (0.564 g, 2.37 mmol). After stirring the solution for 10 min, ethanol was added (15 cm^3) and the reaction mixture was heated to concentrate. During the heating a green precipitate formed; it was filtered off, washed with ethanol and dried in air (yield 84%).

$[NiBr_2(pydz)]$ **2**. Reagent: $NiBr_2\cdot3H_2O$. The same pale green complex was obtained both from ethanolic and aqueous solution (yields *ca.* 50%) (Found: C, 16.75; H, 1.75; N, 9.55. Calc. for $C_4H_4Br_2N_2Ni$: C, 16.10; H, 1.35; N, 9.40%). Room-temperature μ_{eff} 3.3 μ_B. Main IR bands (cm^{-1}): 1578s, 1451m, 1405s, 1077s, 994s, 760vs and 680m.

$[MnCl_2(pydz)]$. Reagent: $MnCl_2\cdot4H_2O$. Yield 94% (Found: C, 23.55; H, 2.00; N, 13.30. Calc. for $C_4H_4Cl_2MnN_2$: C, 23.35; H, 1.95; N, 13.60%). The white product exhibits a room-temperature μ_{eff} of 5.6 μ_B. Main IR bands (cm^{-1}): 1575s, 1455s, 1414s, 1394m, 1224m, 1071s, 990s, 766s and 677m.

$[MnBr_2(pydz)]$. Reagent: $MnBr_2\cdot4H_2O$. Yield 81% (Found: C, 17.35; H, 1.60; N, 9.30. Calc. for $C_4H_4Br_2MnN_2$: C, 16.30; H, 1.40; N, 9.50%). The white product has a room-temperature μ_{eff} of 5.4 μ_B. Main IR bands (cm^{-1}): 1575s, 1455m, 1415s, 1394m, 1221m, 1067s, 984s, 760vs and 673s.

$[FeCl_2(pydz)]$. Reagent: $FeCl_2\cdot4H_2O$. Yield 85% (Found: C, 23.90; H, 1.95; N, 13.25. Calc. for $C_4H_4Cl_2FeN_2$: C, 23.20; H, 1.95; N, 13.55%). The product is brown and has a room-temperature μ_{eff} of 4.9 μ_B. Main IR bands (cm^{-1}): 1575s, 1451s, 1414vs, 1067s, 990s, 760vs and 677m.

$[FeBr_2(pydz)]$. Reagent: $FeBr_2$. The reaction was performed in a Schlenk-tube apparatus under a nitrogen atmosphere. Iron(II) bromide (0.501 g, 2.32 mmol) was dissolved in ethanol (40 cm^3). An insoluble residue was then filtered off. The base was added (0.160 cm^3, 2.20 mmol) with stirring and the solution left to react for 1 h. The brown product formed was filtered off and washed with ethanol. It analysed for the 1 : 1 adduct $[FeBr_2(pydz)]$, but its powder diffraction pattern showed only an amorphous halo. On evaporating the mother-liquor to dryness a microcrystalline dark brown product was recovered (0.440 g), which showed strict analogies with the other bromides of this series, both in IR and XRPD spectra. Unfortunately, an analytically pure sample could not be obtained, as repeated analyses, after thorough washings, always showed the presence of variable amounts of pyridazine as impurity.

$[CoCl_2(pydz)]$. Reagent: $CoCl_2\cdot6H_2O$. Yield 49% (Found: C, 23.30; H, 2.05; N, 13.05. Calc. for $C_4H_4Cl_2CoN_2$: C, 22.90; H, 1.90; N, 13.35%). The product is violet and presents a room-temperature μ_{eff} of 4.9 μ_B. Main IR bands (cm^{-1}): 1581s, 1457m, 1414s, 1227m, 1074s, 1000s, 763vs and 683m.

$[CoBr_2(pydz)]$. Reagent: $CoBr_2\cdot H_2O$. Yield 63% (Found: C, 16.65; H, 1.35; N, 10.05. Calc. for $C_4H_4Br_2CoN_2$: C, 16.10; H, 1.35; N, 9.40%). The pale green product exhibits a room-temperature μ_{eff} of 4.9 μ_B. Main IR bands (cm^{-1}): 1578s, 1454s, 1414s, 1394s, 1071s, 987s, 760vs and 678m.

$[CuCl_2(pydz)]$. Reagent: $CuCl_2\cdot2H_2O$. Yield 83% (Found: C, 22.90; H, 2.20; N, 12.60. Calc. for $C_4H_4Cl_2CuN_2$: C, 22.40; H, 1.90; N, 13.05%). The green product exhibits a room-temperature μ_{eff} of 1.7 μ_B. Main IR bands (cm^{-1}): 1574m, 1457m, 1405s, 1073s, 1007s, 765vs and 680s. The product was obtained also from water solution.

$[CuBr_2(pydz)]$. Reagent: $CuBr_2$. Yield >97% (Found: C, 16.15; H, 1.20; N, 9.25. Calc. for $C_4H_4Br_2CuN_2$: C, 15.85; H, 1.35; N, 9.25%). The product is light brown and has a room-temperature μ_{eff} of 1.7 μ_B. Main IR bands (cm^{-1}): 1575m, 1455m, 1404s, 1074s, 997s, 764vs and 673m. The product was obtained also from water solution.

$[ZnCl_2(pydz)_2]$. Reagent: $ZnCl_2$. Yield 80% (Found: C, 32.40; H, 2.90; N, 18.50. Calc. for $C_8H_8Cl_2N_4Zn$: C, 32.40; H, 2.70; N, 18.90%). The product is white and the main IR bands (cm^{-1}) are at 1575s, 1458m, 1448m, 1424s, 1414s, 1298m, 1284m, 1207m, 1081s, 1071s, 1054m, 977s, 967s, 774vs, 740s and 674s.

$[ZnBr_2(pydz)_2]$. Reagent: $ZnBr_2$. Yield 94% (Found: C, 24.85; H, 1.80; N, 14.40. Calc. for $C_8H_8Br_2N_4Zn$: C, 24.95; H, 2.10; N, 14.55%). The white product exhibits the following main IR bands (cm^{-1}): 1575s, 1451s, 1419s (br), 1297m, 1204m, 1077s, 1071s, 1054s, 980s, 967s, 774vs, 740s and 673s.

X-Ray Powder Diffraction Analysis.—X-Ray powder diffraction data were obtained with Cu-Kα radiation (λ = 1.5418 Å) on a Rigaku D-III MAX horizontal-scan powder diffractometer equipped with parallel Soller slits, a graphite monochromator in the diffracted beam, a Na(Tl)I scintillation counter and pulse-height amplifier discrimination. The generator was operated at 40 kV and 30 mA. Slits used: (divergence) 1.0°, (antiscatter) 1.0°, (receiving) 0.3°.

The powders of complexes **1** and **2** were gently ground in an agate mortar, in order to ensure homogeneity in particle size, then cautiously deposited on a quartz monocrystal, cut along the 511 direction (zero background sample holder, supplied by The Gem Dugout, State College, PA), with the aid of a binder (5% collodion in amyl acetate). The data were collected, at room temperature, in the 5–105° (2θ) range, in the θ–2θ mode, step scan width Δ(2θ) 0.02° and fixed time 10 s.

Standard peak-search methods were used for location of the diffraction maxima, which were then fed to the trial-and-error indexing program TREOR.[29] All mono- and di-metric systems were unsuccessfully tested. In the case of the bromine derivative the program found a reasonable agreement within the orthorhombic system with a = 7.553, b = 6.810, c = 12.913 Å and figures of merit $M(12) = 23$,[30] $F(12) = 20$ (0.013, 45).[31]

In the case of complex **1** TREOR found a cell with half the volume of that of **2** [a = 3.671, b = 6.600, c = 12.723 Å and $M(13) = 26$, $F(13) = 23$ (0.018, 31)]. Density considerations lead to a Z value of 2 for **1** and 4 for **2**. However, a detailed analysis of the systematic absences for **1** did not lead to any reasonable space group, compatible with the unit formula *and* its site symmetries. Therefore, the (short) a axis of **1** was doubled, indicating the probable isomorphous nature of the two compounds. The space group *Imma* was chosen from systematic absences and subsequently confirmed by satisfactory refinement.

The structure solution was first performed on the bromide

Table 1 Crystal data for compounds **1** and **2** *

Compound	**1**	**2**
Formula	$C_4H_4Cl_2N_2Ni$	$C_4H_4Br_2N_2Ni$
M	209.705	298.617
a/Å	7.3758(4)	7.5598(9)
b/Å	6.6069(3)	6.8029(8)
c/Å	12.7292(7)	12.905(2)
U/Å^3	621.43	663.71
D_c/g cm^{-3}	2.241	2.988
F(000)	416	560
No. reflections	454	498
R_p	0.062	0.078
R_{wp}	0.085	0.109
R_F	0.046	0.042

* Details in common: orthorhombic, space group *Imma*; $Z = 4$; 4400 observations; $R_p = \Sigma|y_i - y_{ci}|/\Sigma y_i$, $R_{wp} = [\Sigma w_i(y_i - y_{ci})^2/\Sigma w_i y_i^2]^{\frac{1}{2}}$, $R_F = \Sigma|F_o - F_c|/\Sigma F_o$, where y_i and y_{ci} are the observed and calculated intensities at the ith step (without background subtraction), respectively, w_i is a weighting factor (taken as $w_i = 1/y_i$) and F_o and F_c are the 'observed' and calculated structures factors for all the allowed reflections.

derivative since the larger scattering power of the bromine atom made the tasks of locating the heavy atoms (Ni, Br) easier. The ALLHKL program[32] was used to extract integrated intensities for 77 space-group-allowed reflections in the 2θ 5–65° range. These were then used in the direct-methods package specifically developed for powder data, SIRPOW,[33] which, after a few cycles, provided the initial atomic coordinates for Ni, Br and N and an R factor of 0.09. At this stage, the (expected) polymeric nature of the compound was clear. The correctness of the position of these atoms were confirmed by successful refinement, with the DBW 3.2 program,[34] down to $R_p = 0.11$. The missing C atoms of the pyridazine ligand were then added in ideal positions as a starting model. The same model was then used for the chloride compound, for the two unit cells previously found showed marked analogies.

The two structures were ultimately refined using the Rietveld technique and the GSAS package,[35] which allows the possibility of constraining geometrical parameters to known values. In the final runs the low-angle data (2θ < 17°), *i.e.* those affected most by instrumental aberrations, were discarded. A detailed description of the experimental procedure and data analysis can be found in ref. 27. A total of 4400 data points from each pattern were then used in the final cycles. All bond distances and angles within the pyridazine groups were set at 1.37 Å and 120°, respectively. Two sets of isotropic thermal parameters were used, one for the metal atoms and one for their ligands. The contribution of the hydrogen atoms to the structure factors was neglected. Atomic scattering factors were taken from the internal GSAS library. Final R_p, R_{wp} and R_F values were 0.062, 0.085, 0.040 for complex **1** and 0.078, 0.109, 0.042 for **2**, with 454 and 498 reflections, respectively. Fig. 1 shows the observed and calculated diffraction patterns for **1** and **2**. Crystal data and details on the refinements are collected in Table 1, final fractional atomic coordinates in Table 2.

Results and Discussion

Preparation of the Compounds.—All adducts (but one) were prepared by reaction at room temperature in the air of the appropriate metal salt dissolved in ethanol with an equimolar amount of the pydz base, in line with previously described syntheses.[8,9,12] A precipitate was rapidly obtained in all cases, which was filtered off, washed with ethanol and dried in air. The nickel and copper species were also prepared from water solutions, which give, especially in the case of Ni, slightly slower yields. The aim was to obtain single crystals of the nickel species. However, the products obtained under these conditions are the same as those prepared from ethanol solutions, and their microcrystalline nature prevented any single-crystal X-ray analysis.

As previously observed,[8,9,12] the zinc derivatives obtained under these conditions have a different nature, the elemental analyses being indicative of a metal : pydz ratio of 1 : 2. This is confirmed by their different powder diffraction patterns (see below).

A peculiar problem concerns the preparation of the $FeBr_2$ adduct. This species is very elusive and, accordingly, had not been previously described. Attempts to prepare it in ethanol solution in the open air, as described above for the other species, gave an uncharacterized product, with an elemental analysis close to that expected for a 1 : 1 adduct, but with a complex and completely different powder diffraction pattern and a room-temperature magnetic susceptibility much lower than that for a iron(II) complex having the expected formulation. Oxidation to Fe^{III} may have occurred under these conditions. On performing the reaction in ethanol under a nitrogen atmosphere it was possible to isolate, serendipitously, a dark material isomorphous with the corresponding chloride (see Experimental section).

The compounds are air-stable species, insoluble in common organic solvents. The nickel and copper products are also insoluble in water. The room-temperature magnetic susceptibilities and IR spectra are in substantial agreement with previously reported data.[8,11,12]

Crystal Chemistry.—The complexes $[NiX_2(pydz)]$ (X = Cl or Br) consist of infinite polymeric chains of (octahedral) *trans*-D_{4h} NiX_4N_2 chromophores sharing (four) μ-X and (two) μ-pyridazine ligands (see Fig. 2). Rietveld refinements of XRPD spectra obtained from laboratory equipment normally afford individual bonding parameters either too imprecise or restrained to be close to sound literature values. However, the refined bond distances and angles should still be indicative of the nature of the bonding interactions when relative to 'heavy' atoms. Relevant bond parameters for complexes **1** and **2** are collected in Table 3 and a comparison with pertinent literature values shows that they are reasonable. The Ni–Cl and Ni–Br bond distances are virtually identical to the average values for μ-bridging halogens in six-co-ordinate derivatives (2.422 *vs.* 2.426 and 2.560 *vs.* 2.554 Å for Cl and Br, respectively).[37] The Ni–N interactions are also well behaved since they fall very close to the average Ni–N bond distance found in octahedral pyridine derivatives.[37] Closer comparisons are forbidden by the very nature of the problem; to our knowledge, this is the first structural characterization of a $Ni^{II}X_4N_2$ (X = Cl or Br) moiety since such chromophores were systematically found in insoluble polymeric derivatives.[38]

The major output of an *ab initio* XRPD crystal structure determination is the (gross) molecular conformation and the packing motif, which, it is worth noting, are transferable properties common to all isomorphous compounds. Hence, most of the stereochemistry we are going to discuss for the nickel derivatives will also hold for the related phases of manganese, iron and cobalt which we have found (by XRPD, see Table 4) to have similar unit-cell parameters and to possess a common space group.

The polymeric chains present in all these derivatives can be ideally related to the ZrI_3 chain structure[39] with face-sharing octahedra where two *trans* μ-halides have been substituted by a μ-pyridazine-*N*,*N′* ligand. The substitution of a μ-monodentate by a μ-bidentate ligand obviously changes the folding of the octahedra about the common X · · · X hinge and the resulting chain is shown in Fig. 3 (the actual hinge angle between two adjacent NiX_4 moieties is close to 131° while for regular face-sharing octahedra it should be 109.4°). It is worth noting that such folding depends on the bite of the incoming bridging ligand and, as a consequence, can be tuned by selecting a different (flat) diamine.

The chains grow parallel to the b axis (the b parameters are

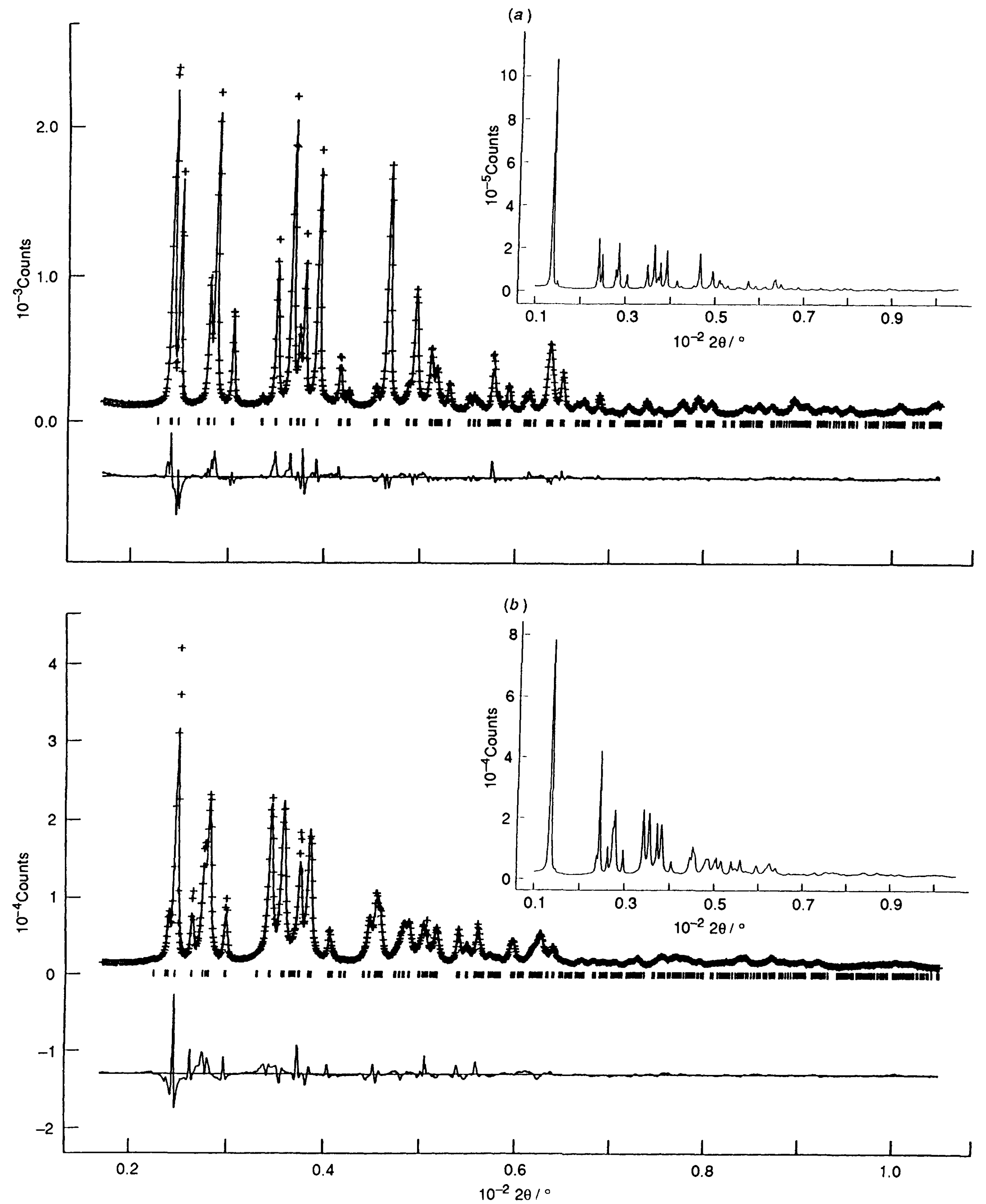

Fig. 1 Observed (+) and calculated (solid line) XRPD patterns for [$NiCl_2$(pydz)] (*a*) and [$NiBr_2$(pydz)] (*b*). Reflection markers and difference plots are at the bottom. The inserts show the complete experimental data.

immediately informative of the intrachain M ⋯ M separation which is equal to $\frac{b}{2}$) and, as shown in Fig. 4 for the [$NiCl_2$(pydz)] derivative, are closely packed in the *ac* plane. Indeed, each chain is pseudo-hexagonally surrounded by six (symmetry-related) chains the baricentres of which describe, in the *ac* plane, an almost regular hexagon with two sides of length *a* and four of *h* (half the diagonal of the *ac* lattice face). As given in Table 4, the *a*:*h* ratio is close to unity for the whole set of isomorphous derivatives. The chains lack, however, a circular profile and their packing is strongly interpenetrated. In this context it is worth noting the stacking, along the *a* direction, of the pyridazine ligands

Table 2 Fractional atomic coordinates for [$NiCl_2$(pydz)] **1** and [$NiBr_2$(pydz)] **2** with estimated standard deviations (e.s.d.s) in parentheses

	1			**2**		
Atom	*X/a*	*Y/b*	*Z/c*	*X/a*	*Y/b*	*Z/c*
Ni	0	0	0	0	0	0
Cl or Br	0.218 8(3)	−0.25	0.057 4(2)	0.230 8(3)	−0.25	0.060 8(2)
N	0	0.146 38(9)	0.144 9(4)	0	0.149 8(4)	0.143 6(9)
C(1)	0	0.042 67(9)	0.238 2(4)	0	0.048 4(4)	0.235 1(10)
C(2)	0	0.146 32(9)	0.331 5(4)	0	0.149 2(4)	0.327 9(10)

Table 3 Selected bond distances (Å) and angles (°) for [$NiCl_2$(pydz)] **1** and [$NiBr_2$(pydz)] **2** with e.s.d.s in parentheses

	1	**2**
Ni–X	2.422(1)	2.560(2)
Ni–N	2.083(5)	2.115(11)
X···X	3.227(4)	3.489(5)
X–Ni–X (endocyclic)	83.55(7)	85.92(9)
X–Ni–X (exocyclic)	96.45(7)	94.08(9)
X–Ni–N	92.84(6)	92.9(1)
Ni–X–Ni	86.00(6)	83.27(7)
Ni–N–N	117.67(7)	118.8(2)
NiX_4/NiX_4 Hinge	132.27(5)	130.43(5)

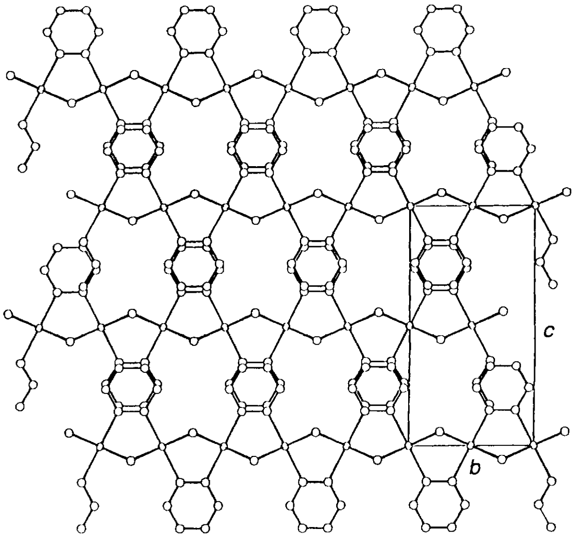

Fig. 2 An ORTEP[36] drawing of the [$NiCl_2$(pydz)] polymer, viewed down the *a* axis

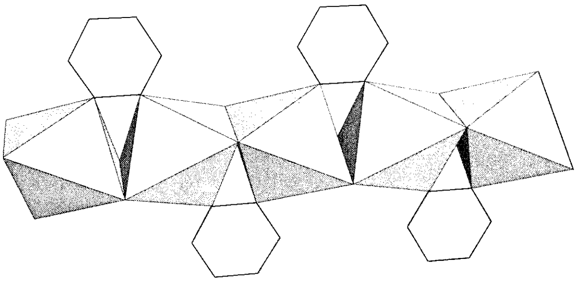

Fig. 3 An ATOMS[40] drawing of a single [$NiCl_2$(pydz)] chain; the $NiCl_4N_2$ co-ordination octahedra are shaded

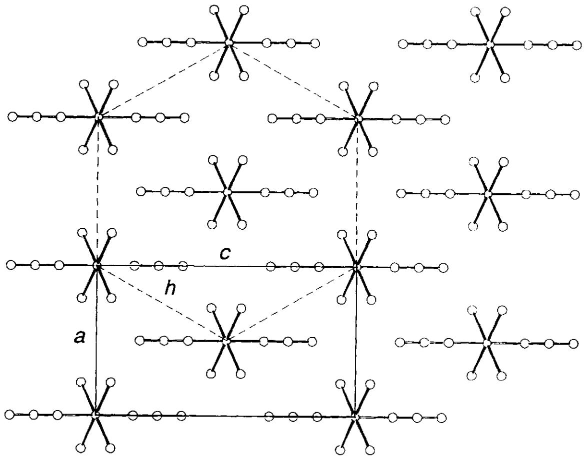

Fig. 4 Crystal packing of the [$NiCl_2$(pydz)] chains, viewed down the *b* axis, showing the pseudo-hexagonal arrangement of the chains in the *ac* plane

(Figs. 2 and 4), the distance characterizing such 'graphitic' interactions being $\frac{a}{2}$.

A close analysis of the crystallographic data in Table 4 shows that all the bromides are isomorphous with the corresponding chlorides and that the derivatives of Mn, Fe, Co and Ni have similar unit-cell parameters and a common space group while those of Cu and Zn do not. Moreover the lattice parameter *b*, which is directly related to the M···M distance, is the most sensitive to 'chemical' perturbations. In particular, on moving from the chloride to the bromide derivatives there is a larger (percentage) variation of *a* and *b* with respect to *c*. However, on changing the metal in the sequence Ni, Co, Fe, Mn there is a larger variation of *b* with respect to *a* and *c* (and a systematic expansion of the cell volume). These facts allow the following generalizations: (*i*) the 'short' M···M distances are essentially the result of the steric requirements of the bridging ligands and are not indicative *per se* of the presence of M···M interactions; (*ii*) the stacking distance of the pyridazine rings depends on the 'lateral thickness' of the chains, *i.e.* on the out-of-plane displacements of the halogen atoms; (*iii*) the relative size of the Ni, Co, Fe and Mn atoms in the present derivatives is better accounted for by Shannon crystal radii [high-spin metal(II) species], which smoothly increase in the above order, rather than by covalent radii, which have an erratic behaviour for such atoms.

The complex [$CuCl_2$(pydz)] has been previously characterized[18] by single-crystal X-ray diffraction in the *C*2/*c* space group (unique axis *b*). The simple linear transformation (1,− 1,0; 0,0,1; 0,1,0), which allows one to describe this structure in the non-standard space group *I*2/*b* (unique axis *c*) discloses the structural relationship between the orthorhombic (Ni, Co, Fe, Mn) derivatives and the monoclinic copper one. The *I*2/*b* cell parameters are all close to the corresponding *Imma* ones, with the obvious exception of the angle γ. The refined atomic coordinates are also similar for the derivatives of Ni and Cu. Accordingly, we might conclude that the derivatives of Ni, Co, Fe, Mn and Cu share a common structural motif which is, however, perturbed, in the copper case, by a Jahn–Teller distortion, which transforms the almost regular octahedral co-ordination (of the Ni, Co, Fe and Mn atoms) into a tetragonally distorted one (for Cu). The major effects of such distortion are

Table 4 Summary of lattice parameters of the $[MX_2(pydz)]$ series (M = Mn, Fe, Co, Ni, Cu or Zn; X = Cl or Br)

$[MCl_2(pydz)]$

	Mn	Fe	Co	Ni	Cu	Zn
Space group	*Imma*	*Imma*	*Imma*	*Imma*	*I*2/*b*[a,b]	Orthorhombic *P*
a/Å	7.428	7.349	7.343	7.376	7.402	7.72
b/Å	6.868	6.712	6.690	6.607	6.757	11.74
c/Å	13.013	12.933	12.865	12.729	12.429	12.77
γ/°					97.13	
h/Å	7.492	7.438	7.406	7.356	—	—
h:*a*	1.009	1.012	1.008	0.997	—	—
U/Å^3	663.9	638.0	632.0	621.4	616.9	1142

$[MBr_2(pydz)]$

	Mn	Fe	Co	Ni	Cu	Zn
Space group	*Imma*	*Imma*	*Imma*	*Imma*	*I*2/*b*[a,c]	Orthorhombic *P*
a/Å	7.776	7.676	7.592	7.560	7.708	7.78
b/Å	7.095	6.951	6.899	6.803	6.928	11.99
c/Å	13.207	12.981	12.988	12.905	12.597	12.89
γ/°					97.26	
h/Å	7.663	7.540	7.522	7.478	—	—
h:*a*	0.985	0.982	0.991	0.989	—	—
U/Å^3	728.6	692.6	680.3	663.7	667.3	1202

[a] Non-standard setting of *C*2/*c* (see ref. 18). [b] $a = 9.383$, $b = 12.429$, $c = 6.757$ Å; $\beta = 128.48°$. [c] $a = 9.691$, $b = 12.597$, $c = 6.928$ Å; $\beta = 127.91°$.

the asymmetrization of the bridging Cl atoms (which eventually affords four M–Cl interactions, two stronger and two weaker than the original ones) and the lowering of the space-group symmetry from *Imma* to its subgroup *I*2/*b*.

Chemical analysis and cell volumes indicate that the two zinc derivatives can be formulated as $[ZnX_2(pydz)_2]$ (X = Cl or Br); work is in progress to ascertain their structure by *ab initio* XRPD techniques.

Conclusion

We have shown that XRPD is a valuable tool for extracting structural information from co-ordination polymer samples. Since solubilization essentially involves chain scission by ligand-exchange reactions, these polymers cannot be characterized spectroscopically in solution; they only exist in the solid state but rarely can be obtained as single crystals or fibres. Accordingly, we have structurally characterized the $[NiCl_2(pydz)]$ and $[NiBr_2(pydz)]$ powders, shown the isomorphous nature of the derivatives of Co, Fe and Mn and evidenced the structural relationships with the copper analogues.

Again, we want to emphasize that the presence of 'rigid' ligands (such as pyrazolates,[27] pyridazine and imidazolates[41]) clearly lowers the structural complexity to be modelled by the powder method by allowing the use of geometrical constraints. However, although a high accuracy level cannot be obtained, the average bond distances, the overall topology, the molecular conformation and crystal packing are well determined.

Acknowledgements

We thank the Italian Consiglio Nazionale delle Ricerche (Progetto Finalizzato: Materiali Speciali per Tecnologie Avanzate) for funding. The assistance of Dr. P. Cremaschi with graphics facilities is also acknowledged.

References

1 (*a*) M. Inoue and M. Kubo, *Coord. Chem. Rev.*, 1976, **21**, 1; (*b*) P. J. Steel, *Coord. Chem. Rev.*, 1990, **106**, 227.

2 See, for example, M. A. Esteruelas, M. P. Garcia, A. M. Lopez and L. A. Oro, *Organometallics*, 1991, **10**, 127 and refs. therein.

3 See, for example, W. Kobel and M. Hanack, *Inorg. Chem.*, 1986, **25**, 103.

4 B. F. Hoskins and R. Robson, *J. Am. Chem. Soc.*, 1990, **112**, 1546.

5 T. Otieno, S. J. Rettig, R. C. Thompson and J. Trotter, *Inorg. Chem.*, 1993, **32**, 1607.

6 G. Spacu, P. Spacu and E. Radulescu, *Chem. Abstr.*, 1959, **58**, 8909(e).

7 C. Reimann and G. Gordon, *Nature* (*London*), 1965, **205**, 902.

8 J. R. Ferraro, C. Cristallini and G. Roch, *Ric. Sci.*, 1967, **37**, 435.

9 J. R. Ferraro, W. Wozniak and G. Roch, *Ric. Sci.*, 1968, **38**, 433.

10 K. Hyde, G. F. Kokoszka and G. Gordon, *J. Inorg. Nucl. Chem.*, 1969, **31**, 1993.

11 J. R. Ferraro, J. Zipper and W. Wozniak, *Appl. Spectrosc.*, 1969, **23**, 160.

12 J. R. Allan, G. A. Barnes and D. H. Brown, *J. Inorg. Nucl. Chem.*, 1971, **33**, 3765.

13 S. Emori, M. Inoue and M. Kubo, *Bull. Chem. Soc. Jpn.*, 1972, **45**, 2259.

14 J. J. Porter, J. L. Murray and K. B. Takvorian, *J. Heterocycl. Chem.*, 1973, **10**, 43.

15 S. A. A. Zaidi and T. A. Khan, *Indian J. Chem., Sect. A*, 1977, **15**, 461.

16 M. D. Child, G. A. Foulds, G. C. Percy and D. A. Thornton, *J. Mol. Struct.*, 1981, **75**, 191.

17 D. P. Drolet, A. J. Lees and A. D. Katnani, *Inorg. Chim. Acta*, 1988, **150**, 197.

18 T. Fetzer, A. Lentz, T. Debaerdemaeker and O. Abou-El-Wafa, *Z. Naturforsch., Teil B*, 1990, **45**, 199.

19 *IUCr Monographs on Crystallography*, Oxford University Press, New York, 1993, vol. 5.

20 G. Will, *Aust. J. Phys.*, 1988, **41**, 283.

21 *Reviews in Mineralogy*, The Mineralogical Society of America, Washington, DC, 1989, vol. 20.

22 D. K. Smith and S. Gorter, *J. Appl. Cryst.*, 1991, **24**, 369.

23 A. Le Bail, H. Duroy and J. L. Fourquet, *Mat. Res. Bull.*, 1988, **23**, 447; A. Le Bail, J. L. Fourquet and U. Bentrup, *J. Solid State Chem.*, 1992, **100**, 151; A. Le Bail, *J. Solid State Chem.*, 1993, **103**, 287; D. Louër, M. Louër and M. Touboul, *J. Appl. Cryst.*, 1992, **25**, 617.

24 K. Honda, M. Goto and M. Kurahashi, *Chem. Lett.*, 1990, 13; R. J. Cernik, A. K. Cheetham, C. K. Prout, D. J. Watkin, A. P. Wilkinson and B. T. M. Willis, *J. Appl. Crystallogr.*, 1991, **24**, 222; P. Lightfoot, M. Tremayne, K. D. M. Harris and P. G. Bruce, *J. Chem. Soc., Chem. Commun.*, 1992, 1012; M. Tremayne, P. Lightfoot, C. Glidewell, K. D. M. Harris, K. Shankland, C. J. Gilmore, G. Bricogne and P. G. Bruce, *J. Mater. Chem.*, 1992, **2**, 1301.

25 J. Fayos, G. Artioli and R. Torres, *J. Crystallogr. Spectrosc. Res.*, 1993, **23**, 595; P. Lightfoot, C. Glidewell and P. G. Bruce, *J. Mater. Chem.*, 1992, **2**, 361; P. Lightfoot, C. Glidewell and P. G. Bruce,

J. Organomet. Chem., 1994, **466**, 51; S. Petit, G. Coquerel, G. Perez, D. Louër and M. Louër, *New J. Chem.*, 1993, **17**, 187; S. Petit, G. Coquerel, G. Perez, D. Louër and M. Louër, *Chem. Mater.*, 1994, **6**, 116.
26 N. Masciocchi, M. Moret, P. Cairati, F. Ragaini and A. Sironi, *J. Chem. Soc., Dalton Trans.*, 1993, 471.
27 N. Masciocchi, M. Moret, P. Cairati, A. Sironi, G. A. Ardizzoia and G. La Monica, *J. Am. Chem. Soc.*, 1994, in the press.
28 N. Masciocchi, P. Cairati, F. Ragaini and A. Sironi, *Organometallics*, 1993, **12**, 4499.
29 P. E. Werner, L. Erikson and M. Westdahl, *J. Appl. Crystallogr.*, 1985, **18**, 367.
30 P. H. De Wolff, *J. Appl. Crystallogr.*, 1968, **1**, 108.
31 G. S. Smith and R. L. Snyder, *J. Appl. Crystallogr.*, 1979, **12**, 604.
32 G. S. Pawley, *J. Appl. Crystallogr.*, 1981, **14**, 357.
33 G. Cascarano, L. Favia and C. Giacovazzo, *J. Appl. Crystallogr.*, 1992, **25**, 310.
34 R. A. Young and D. B. Wiles, *J. Appl. Crystallogr.*, 1982, **15**, 430.
35 A. C. Larson and R. B. Von Dreele, LANSCE, MS-H805, Los Alamos National Laboratory, Los Alamos, NM, 1990.
36 C. K. Johnson, ORTEP, A Fortran Thermal Ellipsoid Plot Program for Crystal Structure Illustrations, Oak Ridge National Laboratory, Oak Ridge, TN, 1971.
37 A. G. Orpen, L. Brammer, F. H. Allen, O. Kennard, D. G. Watson and R. Taylor, *J. Chem. Soc., Dalton Trans.*, 1989, S1.
38 L. Sacconi, in *Comprehensive Coordination Chemistry*, ed. G. Wilkinson, Pergamon, Oxford, 1987, vol. 5, p. 1.
39 A. F. Wells, *Structural Inorganic Chemistry*, Clarendon Press, Oxford, 1975, p. 355.
40 E. Dowty, ATOMS, A Computer Program for Displaying Atomic Structures, version 2.2, Kingsport, TN, 1992.
41 N. Masciocchi, M. Moret, P. Cairati, A. Sironi, G. A. Ardizzoia and G. La Monica, unpublished work.

Received 5th *May* 1994; *Paper* 4/02675F